

Proceeding Paper

# Niobium Oxide and Tantalum Oxide Micro- and Nanostructures Grown Using Material Recovered from Mining Tailings <sup>†</sup>

Belén Sotillo <sup>1</sup>, Lorena Alcaraz <sup>2,\*</sup>, Félix Antonio López <sup>2</sup>, Francisco José Alguacil <sup>2</sup>, Olga Rodríguez <sup>2</sup> and Paloma Fernández <sup>1</sup>

<sup>1</sup> Department of Materials Physics, Faculty of Physics, Complutense University of Madrid, 28040 Madrid, Spain; bsotillo@fis.ucm.es (B.S.); arana@fis.ucm.es (P.F.)

<sup>2</sup> National Center for Metallurgical Research (CENIM), Spanish National Research Council (CSIC), Avda. Gregorio del Amo 8, 28040 Madrid, Spain; f.lopez@csic.es (F.A.L.); fjalgua@cenim.csic.es (F.J.A.); olga.rodriguez@csic.es (O.R.)

\* Correspondence: alcaraz@cenim.csic.es

<sup>†</sup> Presented at the 1st International Electronic Conference on Metallurgy and Metals, 22 February–7 March 2021; Available online: <https://iec2m.sciforum.net/>.

**Abstract:** Niobium and tantalum-based oxides were recovered from mining tailings. These oxides were used as starting material for growing micro- and nanostructures by the evaporation method. The morphology and crystal structure of the final oxides were evaluated using X-ray diffraction (XRD), micro-Raman spectroscopy, and scanning electron microscopy (SEM). After the thermal treatment, microrods of both oxides were obtained, which presented exotic stoichiometries Nb<sub>22</sub>O<sub>54</sub> and K<sub>6</sub>Ta<sub>10.8</sub>O<sub>30</sub>, respectively.

**Keywords:** metals recovery; strategic metals; microstructures grown; mining tailing; niobium oxide; tantalum oxide

**Citation:** Sotillo, B.; Alcaraz, L.; López, F.A.; Alguacil, F.J.; Rodríguez, O.; Fernández, P. Niobium Oxide and Tantalum Oxide Micro- and Nanostructures Grown Using Material Recovered from Mining Tailing. *Mater. Proc.* **2021**, *3*, 1. <https://doi.org/10.3390/IEC2M-09235>

Academic Editor: Eric D. van Hullebusch

Published: 18 February 2021

**Publisher's Note:** MDPI stays neutral with regard to jurisdictional claims in published maps and institutional affiliations.



**Copyright:** © 2021 by the authors. Licensee MDPI, Basel, Switzerland. This article is an open access article distributed under the terms and conditions of the Creative Commons Attribution (CC BY) license (<http://creativecommons.org/licenses/by/4.0/>).

## 1. Introduction

Two main problems faced by the increasingly technological society are the large amount of waste that humans generate and the scarcity of many of the materials used. In this sense, one of the EU's priorities is to promote the transition to a circular economy, where the materials and products manufactured with them remain in the life cycle as long as possible. Nb and Ta are highly appreciated metals due to the several technological applications in high-strength alloys, capacitors, supercapacitors [1], catalysis [2], coatings or light guiding [3], electrochemical energy storage devices [4,5], among others. However, the most important problem is that they are scarcely found in the Earth's crust as raw materials. It is thus an interesting topic for the scientific community, to develop new technologies to assure the sustainable use of these raw materials, as well as to improve the processes to recover and recycle them. Due to their importance in high-tech products and emerging innovations, niobium (Nb) and tantalum (Ta) are included in the 2020-year list of the 30 critical raw materials of the European Union [6].

Both Nb and Ta are found as a columbotantalite mineral in nature. This mineral can be extracted from mining tailings [7,8], as in the case of Sn-Nb-Ta concentrate extracted from the Penouta mine (Galicia, Spain). However, the low concentration of both metals, along with their strong association with cassiterite (SnO<sub>2</sub>), and the similar physical and chemical properties of Nb and Ta, has fostered the development of tailored procedures to extract and separate them.

In the present work, powders of these two strategic metals oxides, niobium and tantalum, were recovered from the tailings of the Penouta Sn-Ta-Nb deposit (located in Galicia, Spain) via the hydrometallurgical route [7,8]. The recovered oxide powders were

used to obtain micro- and nanostructures by a thermal evaporation method. The structures were characterized using scanning electron microscopy (SEM), X-ray diffraction (XRD), and micro-Raman spectroscopy. It was shown that the rods grown from the mine-recovered oxide powders have exotic stoichiometries ( $\text{Nb}_{22}\text{O}_{54}$  and  $\text{K}_6\text{Ta}_{10.8}\text{O}_{30}$ , respectively), rarely studied in the literature.

## 2. Materials and Methods

The starting material (cassiterite and columbotantalite) was recovered from mining deposits of the Penouta mine (Galicia, Spain). Initially, mining tailings were treated by a pyrometallurgical process in order to obtain a metal tin ingot and a vitreous slag, as previously reported [7,8]. The slag was milled, and it was leached using a  $\text{HF}/\text{H}_2\text{SO}_4$  mixture for 1 h. Next, the acid mixture was filtered, and extraction of the strategic metals was performed. For this purpose, the leaching liquid phase was put in contact with a mix of 35% (*v/v*) Cyanex 923<sup>®</sup> diluted in Solvesso, where niobium and tantalum were extracted into the organic phase with yields of around 98%. Then, this organic phase was treated to carry out a selective separation of both strategic metals: First, it was stripped with  $\text{NH}_4\text{F}/\text{NH}_3$  (0.27 M/0.106 M), where niobium was extracted to the aqueous phase; subsequently, a  $\text{NH}_4\text{F}/\text{NH}_3$  (1.08 M/0.42 M) was added to the secondary organic phase, and the tantalum in the aqueous phase was recovered [7,8]. Once the Nb and Ta were separated, the corresponding aqueous solutions were precipitated using  $\text{NH}_3$  (concentrate, 17.7 M) and  $\text{KF}$  (90 g/L), respectively. After this process, hydrated Nb oxide ( $\text{Nb}_2\text{O}_5 \cdot n\text{H}_2\text{O}$ ) and  $\text{K}_{0.4}\text{Ta}_{2.4}\text{F}_{0.6}$  compounds were collected. In order to reach the corresponding solid oxide precursors, both Nb and Ta precipitates were calcinated in a tubular furnace at 1200 °C. The procedure to obtain the different samples is shown in Figure 1. Further details of this process can be found in [8].

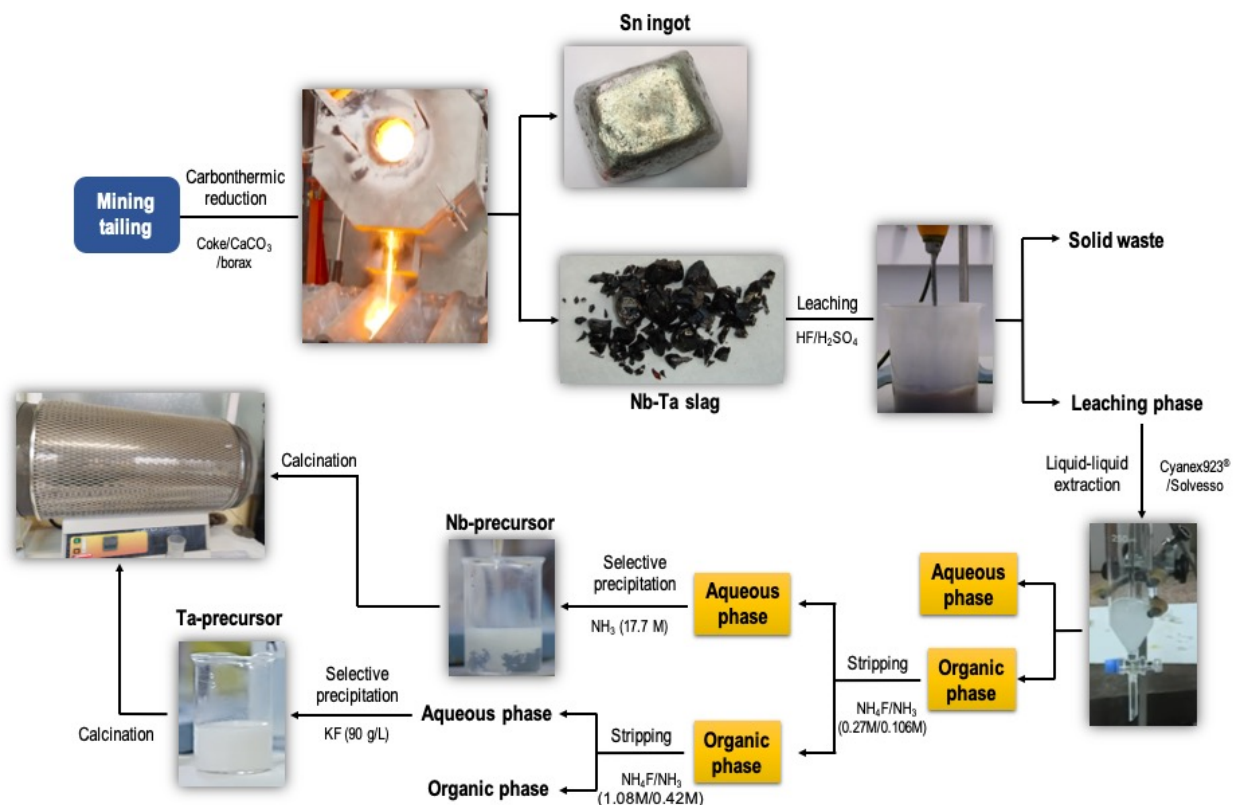


**Figure 1.** Schematic procedure realized to obtain the corresponding niobium and tantalum precursor oxides.

Once niobium and tantalum oxide powders were recovered, they were used to grow microstructures. The powders were placed on an alumina boat and inside a furnace. Then,

the powders were subjected to thermal treatment, with different conditions depending on the precursor. For niobium oxide, the best condition to grow microstructures was 1300 °C during 10 h with an Ar flux. On the other hand, for the tantalum oxide, the treatment to obtain the microstructures was 1500 °C during 8 h under a continuous Ar flux.

The morphology of the recovered powders and of the grown microstructures was studied using two scanning electron microscopes: An FEI Inspect and a Hitachi TM3000 SEM. The structural characterization was carried out through X-ray diffraction (XRD) and micro-Raman spectroscopy ( $\mu$ -Raman). XRD measurements were performed in a PANalytical Empyrean diffractometer (Cu-K $\alpha$  radiation). For performing the  $\mu$ -Raman measurements, a confocal microscope Horiba JobinYvon LABRAM-HR was employed. The excitation wavelength was 632.8 nm from a He-Ne laser. The laser was focused onto the sample with a 100 $\times$  Olympus objective, and the scattered light was also collected using the same objective (backscattering configuration). Further details of the characterization can be found in [8–10].

### 3. Results and Discussion

#### 3.1. Scanning Electron Microscopy (SEM)

The morphology of the recovered oxide powders (as obtained after the procedure shown in Figure 1) is shown in the SEM images of Figure 2a,b. As can be appreciated, irregularly shaped particles were obtained in both cases after the recovery process. In the case of tantalum oxide, some rod-type particles can be identified (Figure 2b). It was only after the thermal treatments when a high density of microrods could be observed. They typically have rectangular sections, as shown in the corresponding SEM micrographs in Figure 2c,d.

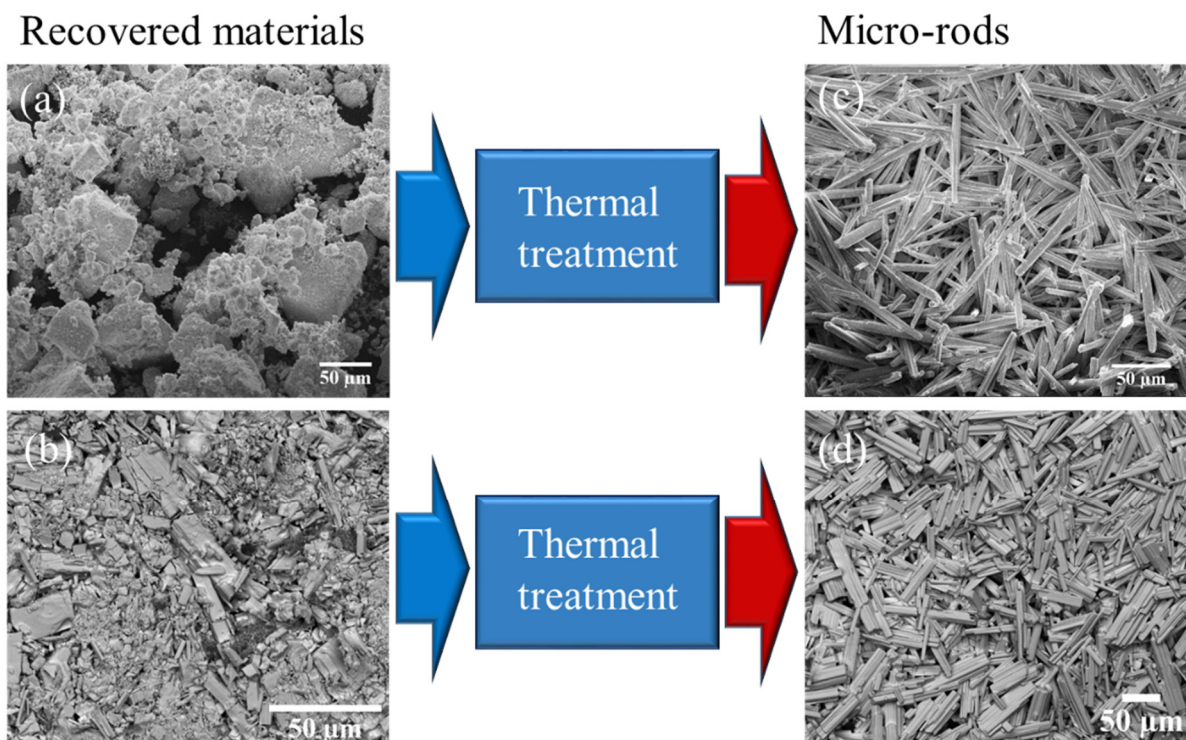


**Figure 2.** SEM micrographs of the niobium and tantalum compounds: (a) SEM of the niobium oxide powders and (b) tantalum-based oxide powders recovered after the procedure indicated in Figure 1. After a thermal treatment of the recovered materials, Ar flux microrods were obtained: (c) SEM image of niobium oxide and (d) tantalum-based oxide rods.

#### 3.2. X-ray Diffraction (XRD)

Upon the thermal treatment, a phase transformation was observed in niobium oxide. The powders recovered after the process shown in Figure 1 were mainly in the pseudo-

hexagonal phase (TT) of  $\text{Nb}_2\text{O}_5$  (Figure 3a, inset). The most intense reflection was indexed to this phase (ICDD No. 00-028-0317). Some less intense peaks can be ascribed to a  $\text{Nb}_{12}\text{O}_{29}$  nonstoichiometric monoclinic phase (ICDD No. 04-014-6587) and quartz impurities, but the results indicate that it was possible to recover niobium oxide compounds. After the thermal treatment at 1300 °C, the main phase registered was  $\text{Nb}_{22}\text{O}_{54}$  (monoclinic phase, ICDD No. 04-014-9203). This information was extracted from the XRD pattern shown in Figure 3a.

On the other hand, no phase transformation was produced in the tantalum oxide material during the thermal treatment. The most intense reflection maxima in the XRD pattern (Figure 3b, inset) can be indexed to the tetragonal tungsten bronze-like structure of  $\text{K}_6\text{Ta}_{10.8}\text{O}_{30}$  (ICDD No. 01-070-1080). These results indicated that the procedure was not able to remove the potassium from the crystal structure of the recovered material. The XRD pattern after the treatment at 1500 °C (Figure 3b) exhibited diffraction maxima according to the same  $\text{K}_6\text{Ta}_{10.8}\text{O}_{30}$  tetragonal tungsten bronze-like structure. This result reveals that this material does not transform its crystal phase as previously described in [8].

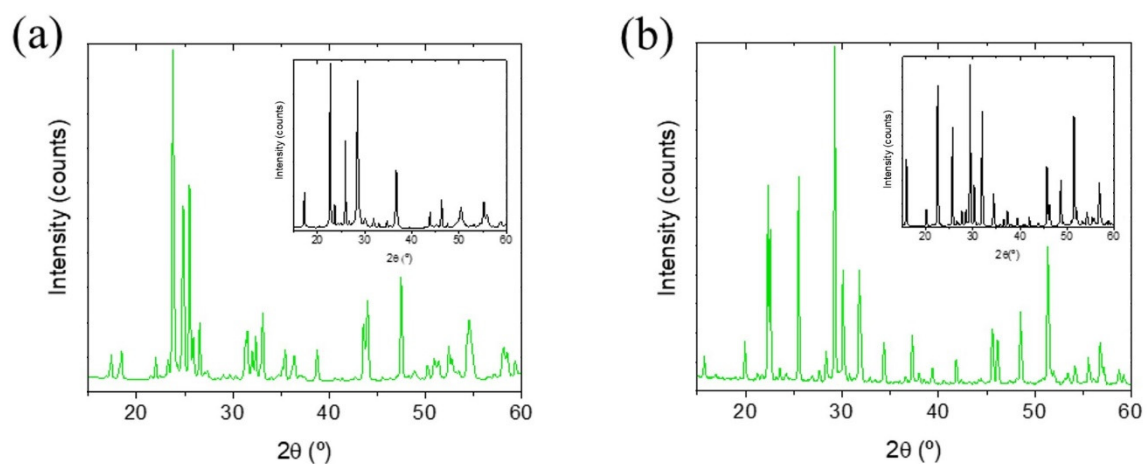


**Figure 3.** Comparison of the XRD patterns taken on the rods of (a) niobium oxides and (b) tantalum-based oxides. In the insets, the XRDs of the initial recovered materials are shown.

The crystal structures obtained in this work may be useful in the fabrication of energy storage devices, as they have crystallographic channels or tunnels where the insertion of ions is possible without producing a large alteration of the volume [11]. In addition, the obtained rods show a high value of refractive index [9,10], as expected for these oxides.

### 3.3. $\mu$ -Raman Spectroscopy

Further studies of the crystal structure of the niobium and tantalum oxides were performed using  $\mu$ -Raman spectroscopy (Figure 4). For both niobium and tantalum oxides, the crystal structures can be seen as a weave of corner-linked  $\text{XO}_6$  octahedra ( $X = \text{Nb}$  or  $\text{Ta}$ ). Most of the observed bands in the Raman spectra can be related to the internal modes of  $\text{XO}_6$  polyhedra [12,13]. The  $200\text{ cm}^{-1} < \nu < 450\text{ cm}^{-1}$  region would correspond to the bending-related modes of the  $\text{XO}_6$  octahedra, while in the  $450\text{ cm}^{-1} < \nu < 900\text{ cm}^{-1}$  region, the modes related to the stretching vibrations of the X-O bonds in the  $\text{XO}_6$  octahedra would be found. Typically, the external lattice vibrations (for which the octahedra is considered as a rigid unit) are found at  $\nu < 200\text{ cm}^{-1}$ . The sharp mode observed at  $520\text{ cm}^{-1}$  corresponds to the silicon substrate.

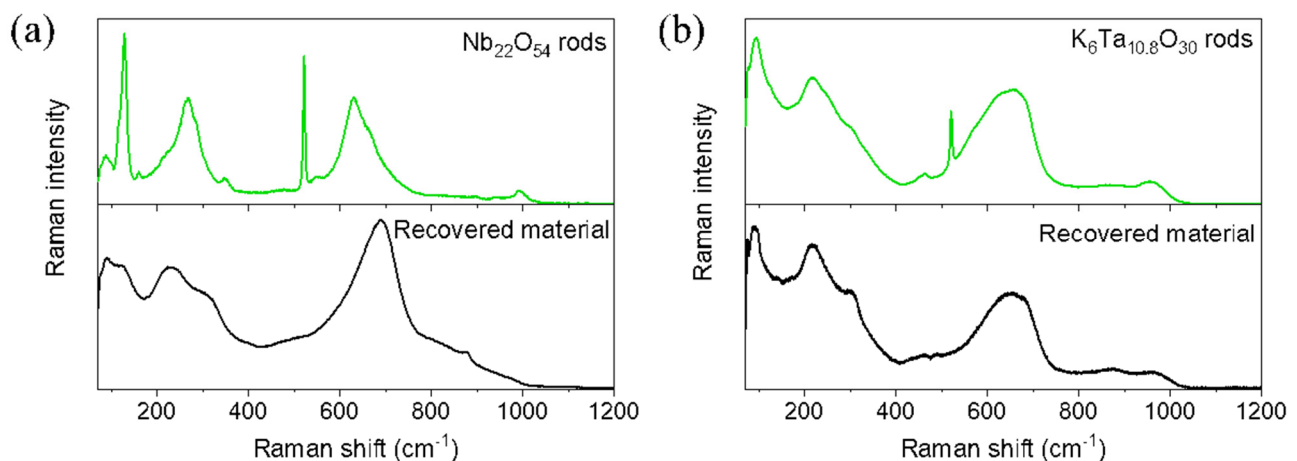


**Figure 4.**  $\mu$ -Raman spectra recorded on the recovered materials, as well as on the microrods: (a) niobium oxide; (b)  $K_6Ta_{10.8}O_{30}$ .

In the case of niobium oxide material (Figure 4a), differences between the recovered material and the rods were detected in the Raman spectra. The bands observed in the recovered material are those expected for the TT-Nb<sub>2</sub>O<sub>5</sub> phase. On the other hand, the rods presented modes that are associated with monoclinic phases (as it is the Nb<sub>22</sub>O<sub>54</sub> compound). The displacement in the band at around 690 cm<sup>-1</sup> toward lower wavenumbers indicates an increasing bond order of octahedra and a more ordered crystal structure. In addition, some of the peaks were sharper than in the recovered material, in agreement with this increase in the crystal order. The new band at 993 cm<sup>-1</sup> is associated with the symmetric stretching modes of the terminal bonds of Nb=O in NbO<sub>6</sub> octahedra.

As expected, in the case of  $K_6Ta_{10.8}O_{30}$  material (Figure 4b), no strong changes were observed between the recovered powders and the rods, as no phase transformation was produced.

A detailed description of the physical properties of the obtained microrods for both materials can be found in [10] (Nb<sub>22</sub>O<sub>54</sub>) and in [9] ( $K_6Ta_{10.8}O_{30}$ ).

#### 4. Conclusions

In the present work, a process to obtain micro- and nanostructures of niobium and tantalum oxides from mining tailings was described. Pyrometallurgical treatment, followed by a selective liquid–liquid extraction and a subsequent precipitation, were used to obtain Nb and Ta precursors. These solids precursors were treated in a furnace under Ar flux to grow the corresponding structures.

**Author Contributions:** B.S.: conceptualization, data curation, formal analysis, investigation, methodology, validation, writing—original draft, writing—review editing. L.A. and O.R.: investigation, methodology, writing—original draft, writing—review editing. F.A.L. and F.J.A.: conceptualization, funding acquisition, project administration, resources, writing—review editing. P.F.: conceptualization, formal analysis, funding acquisition, project administration, resources, writing—review editing. All authors have read and agreed to the published version of the manuscript.

**Funding:** This project has received funding via the projects ESTANNIO (RTC-2017-6629-5) and MINECO/FEDER-MAT2015-65274-R and from the European Union’s Horizon 2020 research and innovation program under grant agreement No. 776851 (Car-E Service).

**Institutional Review Board Statement:** Not applicable.

**Informed Consent Statement:** Not applicable.

**Data Availability Statement:** Not applicable.

**Acknowledgments:** B. Sotillo acknowledges financial support from Comunidad de Madrid (Ayudas del Programa de Atracción de Talento (2017-T2/IND-5465). The authors would like to thank the UCM CAI of X-ray diffraction for performing the XRD measurements.

**Conflicts of Interest:** The authors declare no conflict of interest.

## References

1. Liao, J.; Ni, W.; Wang, C.; Ma, J. Layer-structured niobium oxides and their analogues for advanced hybrid capacitors. *Chem. Eng. J.* **2020**, *391*, 123489, doi:10.1016/j.cej.2019.123489.
2. Zhao, Y.; Zhou, X.; Ye, L.; Chi Edman Tsang, S. Nanostructured Nb<sub>2</sub>O<sub>5</sub> catalysts. *Nano Rev.* **2012**, *3*, 17631, doi:10.3402/nano.v3i0.17631.
3. Nico, C.; Monteiro, T.; Graça, M.P.F. Niobium oxides and niobates physical properties: Review and prospects. *Prog. Mater. Sci.* **2016**, *80*, 1–37, doi:10.1016/j.pmatsci.2016.02.001.
4. Ye, W.; Yu, H.; Cheng, X.; Zhu, H.; Zheng, R.; Liu, T.; Long, N.; Shui, M.; Shu, J. Highly efficient lithium container based on non-Wadsley-Roth structure Nb<sub>18</sub>W<sub>16</sub>O<sub>93</sub> nanowires for electrochemical energy storage. *Electrochim. Acta* **2018**, *292*, 331–338, doi:10.1016/j.electacta.2018.09.169.
5. Zhu, H.; Cheng, X.; Yu, H.; Ye, W.; Peng, N.; Zheng, R.; Liu, T.; Shui, M.; Shu, J. K<sub>6</sub>Nb<sub>10.8</sub>O<sub>30</sub> groove nanobelts as high performance lithium-ion battery anode towards long-life energy storage. *Nano Energy* **2018**, *52*, 192–202, doi:10.1016/j.nanoen.2018.07.057.
6. European Commission. *Study on the Review of the List of Critical Raw Materials—Final Report*; European Commission: Brussels, Belgium, 2020; ISBN 978-92-79-72119-9.
7. López, F.; García-Díaz, I.; Rodríguez Largo, O.; Polonio, F.; Llorens, T. Recovery and Purification of Tin from Tailings from the Penouta Sn–Ta–Nb Deposit. *Minerals* **2018**, *8*, 20, doi:10.3390/min8010020.
8. Rodríguez, O.; Alguacil, F.J.; Baquero, E.E.; García-Díaz, I.; Fernández, P.; Sotillo, B.; López, F.A. Recovery of niobium and tantalum by solvent extraction from Sn–Ta–Nb mining tailings. *RSC Adv.* **2020**, *10*, 21406–21412, doi:10.1039/D0RA03331F.
9. Sotillo, B.; Alcaraz, L.; López, F.A.; Fernández, P. Characterization of K<sub>6</sub>Ta<sub>10.8</sub>O<sub>30</sub> Microrods with Tetragonal Tungsten Bronze-Like Structure Obtained from Tailings from the Penouta Sn-Ta-Nb Deposit. *Nanomaterials* **2020**, *10*, 2289, doi:10.3390/nano10112289.
10. Sotillo, B.; López, F.A.; Alcaraz, L.; Fernández, P. Characterization of Nb<sub>22</sub>O<sub>54</sub> microrods grown from niobium oxide powders recovered from mine tailings. *Ceram. Int.* **2021**, doi:10.1016/j.ceramint.2021.01.252.
11. Han, J.-T.; Liu, D.-Q.; Song, S.-H.; Kim, Y.; Goodenough, J.B. Lithium Ion Intercalation Performance of Niobium Oxides: KNb<sub>5</sub>O<sub>13</sub> and K<sub>6</sub>Nb<sub>10.8</sub>O<sub>30</sub>. *Chem. Mater.* **2009**, *21*, 4753–4755, doi:10.1021/cm9024149.
12. Jehng, J.M.; Wachs, I.E. Structural chemistry and Raman spectra of niobium oxides. *Chem. Mater.* **1991**, *3*, 100–107, doi:10.1021/cm00013a025.
13. Dobal, P.S.; Katiyar, R.S.; Jiang, Y.; Guo, R.; Bhalla, A.S. Raman scattering study of a phase transition in tantalum pentoxide. *J. Raman Spectrosc.* **2000**, *31*, 1061–1065, doi:https://doi.org/10.1002/1097-4555(200012)31:12<1061::AID-JRS644>3.0.CO;2-G.